

Adversarial robustness for latent models: Revisiting the robust-standard accuracies tradeoff

Adel Javanmard* Mohammad Mehrabi*†

October 25, 2021

Abstract

Over the past few years, several adversarial training methods have been proposed to improve the robustness of machine learning models against adversarial perturbations in the input. Despite remarkable progress in this regard, adversarial training is often observed to drop the standard test accuracy. This phenomenon has intrigued the research community to investigate the potential tradeoff between standard and robust accuracy as two performance measures. In this paper, we revisit this tradeoff for latent models and argue that this tradeoff is mitigated when the data enjoys a low-dimensional structure. In particular, we consider binary classification under two data generative models, namely Gaussian mixture model and generalized linear model, where the feature data lie on a low-dimensional manifold. We show that as the manifold dimension to the ambient dimension decreases, one can obtain models that are nearly optimal with respect to both, the standard accuracy and the robust accuracy measures.

1 Introduction

Despite the documented remarkable success of modern machine learning systems, and in particular deep neural networks, in various applications domains, it is well known that these models can be highly vulnerable to adversarially chosen perturbations to the input data at test time. Even more surprisingly, many of such adversarial attacks can be designed to be slight modifications of the input which are seemingly innocuous and imperceptible. For example, in image processing and video analysis there are several examples of adversarial attacks in form of minute pixel-wise perturbations which can significantly degrade the performance of the state-of-the-art classifiers (Szegedy et al., 2014; Biggio et al., 2013); or, in speech recognition where one can design voice commands that are incomprehensible or even completely inaudible to human and can still control the virtual assistant software (Carlini et al., 2016; Vaidya et al., 2015; Zhang et al., 2017).

In response to this fragility, a growing body of work in the past few years has sought to improve the robustness of machine learning systems against adversarial attacks. Despite remarkable progress in designing robust training algorithms and certifiable defenses, it is often observed that these methods compromise the statistical accuracy on unperturbed test data (i.e., test data drawn from the same distribution as training data). Such observation had led prior work to speculate a tradeoff between the two fundamental notions of *robustness* and *generalization* (for a non-exhaustive list see

*Data Sciences and Operations Department, University of Southern California

†The names of the authors are in alphabetical order.

e.g, (Madry et al., 2018a; Raghunathan et al., 2019; Min et al., 2020; Mehrabi et al., 2021)). Some of the promising adversarial training methods, such as TRADES (Zhang et al., 2019) acknowledge such tradeoff by including a regularization parameter which allows to tune between these two measures of performance. There has been also recent line of work (Javanmard and Soltanolkotabi, 2020; Javanmard et al., 2020) which provides precise asymptotic theory for this tradeoff and how it is quantitatively shaped by different components of the learning problem (e.g, adversary’s power, geometry of perturbations set, overparameterization, noise level in training data, etc.) For the setting of linear regression and binary classification it is proved that there is an inherent tradeoff between robustness and standard accuracy (generalization) which holds at population level and for any (potentially computationally intensive) training algorithms (Javanmard et al., 2020; Dobriban et al., 2020; Mehrabi et al., 2021). Nonetheless, these work make strong assumptions on the distribution of data (e.g, Gaussian or Gaussian mixture models), which fail to capture various natural structures in data. This stimulates the following tantalizing question:

() Are there natural data generative models under which the tradeoff between robustness and the standard accuracy (generalization) vanishes, in the sense that one can find models which are performing well (or even optimal) with respect to both measures?*

As a step toward answering this question, Yang et al. (2020) show that when data is well separated, there is no inherent conflict between standard accuracy and robustness. It also provides numerical experiments on a few image datasets to argue that these data are indeed r -well separated for some value r larger than the perturbation radii used in adversarial attacks (i.e., data from different classes are at least r distance apart in the pixel domain.) In (Xing et al., 2021), adversarially robust estimators are studied for the setup of linear regression and a lower bound on their statistical minimax rate is derived. The minimax rate lower bound for sparse model is much smaller than the one for dense model, whereby Xing et al. (2021) argues the importance of incorporating sparsity structure in improving robustness.

The current work takes another perspective towards question (*) by considering the low-dimensional manifold structures in data. Many high-dimensional real-world data sets enjoy low-dimensional structures, and learning low-dimensional representations of raw data is a common task in information processing. In fact, the entire field of dimensionality reduction and manifold learning has been developed around this task. To give concrete examples, the MNIST database of handwritten digits consists of images of size 28×28 (i.e., ambient dimension of 784), while its intrinsic (manifold) dimension is estimated to be ≈ 14 , based on local neighborhoods of data. Likewise, the CIFAR10 database consists of color images of size 32×32 (i.e. ambient dimension of 3,072), but its intrinsic dimension is estimated to be ≈ 35 (Costa and Hero, 2004; Rozza et al., 2012; Spigler et al., 2020). The high-level message of the current work is that the low-dimensional structures in data can mitigate the tradeoff between standard accuracy and robustness, and potentially enable training models that perform gracefully (or even optimal) with respect to both measures.

1.1 Summary of contributions

In this work we focus on two common setups for binary classification, namely Gaussian-mixture model and the generalized linear model, where we also assume that the feature vectors lie on a k -dimensional manifold in a d -dimensional space ($k < d$). We use the ratio d/k as a measure of how structured the data is; larger d/k indicates more structured, while small values of d/k , e.g. the extreme case of $d/k = 1$, indicates that there is no low-dimensional structure in the data. We

assess the generalization property of a model through the notion of *standard risk*, and its robustness against adversarial perturbation through the notion of *adversarial risk* (See Section 2 for formal definition.)

- Under both data generative models, we derive the Bayes-optimal estimators, which provably attain the minimum standard risk. We prove that as $d/k \rightarrow \infty$ then the Bayes-optimal estimator asymptotically achieves the minimum adversarial risk as well. This implies that the tradeoff between robustness and generalization vanishes asymptotically as data becomes more structured.
- While the minimizers of the two risk measures converge to each other as d/k grows, we show that the two risk measures (as functions of estimators) stay away from each other. Specifically, we come up with an estimator for which the standard and adversarial risks remain away from each other by a constant $c > 0$ independent of k, d .
- In Section 3.3, we consider an adversarial training method based on robust empirical loss minimization. While this algorithm is structure agnostic we empirically show that it results in models that are robust and also generalize well. Note that the data structures (distribution), even if not deployed by the training procedure, still comes into picture as the adversarial risk and standard risk are defined with respect to this data distribution.
- We corroborate our theoretical findings with several numerical experiments.

1.2 Related work

There is a growing body of work on the tradeoff between robustness and generalization (see e.g., (Tsipras et al., 2018; Madry et al., 2018b; Zhang et al., 2019; Raghunathan et al., 2019; Yang et al., 2020; Min et al., 2020; Mehrabi et al., 2021)). In particular, Dobriban et al. (2020) consider the isotropic Gaussian-mixture model with two and three classes, and derive Bayes-optimal robust classifiers for ℓ_2 and ℓ_∞ adversaries. This work proves a tradeoff between standard and robust risks which becomes bolder when the classes are imbalanced.

The prior work (Jalal et al., 2017; Song et al., 2018; Stutz et al., 2019) proposed the concept of on-manifold attack, where the adversarial perturbations are done in the latent low-dimensional space. In (Stutz et al., 2019), it is argued that on-manifold adversarial examples are acting as generalization error and adversarial training against such attacks improve the generalization of the model as well. In addition, a so-called on-manifold adversarial training (based on minimax formulation) has been proposed which is similar to the adversarial training method of Madry et al. (2018b) but tailored to perturbations in the manifold space. The subsequent work (Lin et al., 2020) proposes dual manifold adversarial training (DMAT) method which considers adversarial perturbations in both the manifold and the image space to robustify models against a broader class of adversarial attacks. In this terminology, in our current work we consider out-of-manifold perturbations (in the ambient space). Also let us emphasize that (Stutz et al., 2019; Lin et al., 2020) are based on empirical studies on image databases and more on an algorithmic front. The current work contributes to this literature by developing a theory for the role of manifold structure of data in the interplay between robustness and generalization, under specific binary classification setups (viz. Gaussian-mixture model and generalized linear model)

1.3 Notation

For a matrix $W \in \mathbb{R}^{d \times k}$, let $\|W\|$ denote its operator norm, and W^\dagger stand for the Moore–Penrose inverse. Further, let $\kappa(W)$ denote the condition number of W which is defined as $\kappa(W) = \|W\| \cdot \|W^\dagger\|$. Further, let $B_\varepsilon(x)$ denote the ℓ_2 -ball centered at x with radius ε . Throughout the paper, for two functions f, g from integers to positive real numbers, we say $f(n) = o(g(n))$, as n grows to infinity, if for every $\varepsilon > 0$, we can find a positive integer k such that for $n \geq k$, we have $f(n)/g(n) \leq \varepsilon$.

2 Problem Formulation

In the binary classification problem, we are given a set of labeled data points $\{(x_i, y_i)\}_{i=1:n}$ which are drawn i.i.d. from a common law $\mathbb{P}_{x,y}$, where $x \in \mathcal{X} \subset \mathbb{R}^d$ is the feature vector and $y \in \{+1, -1\}$ is the label associated to the feature x . The goal is to predict the label of a new test data point with a feature vector drawn from the similar population. To this end, the learner tries to fit a binary classification model to the training set, which results in an estimated model $\hat{h} : \mathcal{X} \rightarrow \{-1, +1\}$. The conventional metric to measure the accuracy of a classifier h is its average error probability on an unseen data point $(x, y) \sim \mathbb{P}_{x,y}$. This is often referred to as the *standard risk* of the classifier, a.k.a. generalization error. Concretely, standard risk of a classifier h is defined as the following:

$$\text{SR}(h) := \mathbb{P}_{x,y}(h(x)y \leq 0) . \quad (1)$$

Despite the remarkable success in deriving classifiers with high accuracy (low standard risk) during the past decades, it has been observed that even the state-of-the-art classifiers are vulnerable to minute but adversarially chosen perturbations on test data points. In the next section, we introduce *adversarial risk*, as a notion to measure accuracy of classifiers in settings where there is discrepancy between the training and test data distribution.

2.1 Adversarial setup

The adversarial setup can be perceived as a game between the adversary and the learner. First, given access to unperturbed training data, the learner proposes a model h . The adversary observes the model h , and then perturbs each test data point x to x' with perturbation $x - x'$ chosen arbitrarily from a ball with ε -radius. Here, ε is a measure of adversary’s power. Adversarial risk is a metric to measure the model accuracy with respect to such perturbed test data points. In this paper, we consider the ℓ_2 -ball of radius ε for the set of possible perturbations. In this case, the *adversarial risk* of the classifier h is defined as the following:

$$\text{AR}(h) = \mathbb{P}_{x,y} \left(\inf_{\|x'-x\|_{\ell_2} \leq \varepsilon} h(x')y \leq 0 \right) . \quad (2)$$

From the definition of adversarial and standard risk, it can be seen that the standard risk is always not greater than the adversarial risk. The non-negative difference of adversarial and standard risk is referred to as *boundary risk*, and is formulated by

$$\begin{aligned} \text{BR}(h) &:= \text{AR}(h) - \text{SR}(h) \\ &= \mathbb{P}_{x,y} \left(h(x)y \geq 0, \inf_{\|x'-x\|_{\ell_2} \leq \varepsilon} h(x)h(x') \leq 0 \right) . \end{aligned} \quad (3)$$

The boundary risk can be considered as the average vulnerability of the classifier with respect to small perturbations on successfully labeled data points. In other words, it measures the likelihood that the classifier correctly determines the label of a data point, but fails to label another test input very close to the primary data point. In the main result section, we study the boundary risk of optimal classifiers (having the lowest standard risk) in scenarios that feature vectors lie on a low-dimensional manifold. But before proceeding further, we first introduce models with low-dimensional latent structures.

2.2 Latent low-dimensional manifold models

In this paper, we focus on the binary classification problem with high-dimensional features generated from a low-dimensional latent manifold. In this problem, we assume that between the feature vector $x \in \mathbb{R}^d$, and the binary label $y \in \{+1, -1\}$, there exists an inherent low-dimensional link $z \in \mathbb{R}^k$ such that $x \perp\!\!\!\perp y|z$. This structure can be considered as a result of a transformed learning problem, where features of one classification setting with low-dimensional feature z are embedded in a high-dimensional space via a mapping $G : \mathbb{R}^k \rightarrow \mathbb{R}^d$. In this scenario, the learner has access to training data $\{(x_i, y_i)\}_{i=1:n}$, while being oblivious to low-dimensional latent vectors $\{z_i\}_{i=1:n}$.

Throughout the paper, we consider a special case of this model, where $G(z) = \varphi(Wz)$ with $W \in \mathbb{R}^{d \times k}$ is a tall full-rank weight matrix, and φ acting entry-wise on vector inputs with a derivative $d\varphi/dt \geq c$, for some positive constant $c > 0$.

For the reader's convenience, in the next section we provide a summary of well-known results for some widely used binary classification models. This helps us identify the optimal classifier (lowest standard risk) for each setup, and later study their associated boundary risk.

2.3 Classification settings

The focus of this paper is on two widely used binary classification setups: 1) Gaussian mixture model, and 2) generalized linear models which we briefly explain below.

Gaussian mixture models. In the Gaussian mixture model, the binary response value y accepts the positive label with probability p , and the negative label with probability $1 - p$. In this setting, labels are assigned independently from the feature vector z , while feature vectors are generated from a multivariate Gaussian distribution with the mean vector $y\mu$, and a certain covariance matrix. Concretely, the data generating law for the Gaussian mixture problem when features lie on a low-dimensional manifold model of Section 2.2 can be written as the following:

$$y \sim \text{Bern}(p, \{+1, -1\}), \quad x = \varphi(Wz), \quad z \sim \text{N}(y\mu, I_k). \quad (4)$$

In this model, we consider low-dimensional isotropic Gaussian features. In other words, manifold features z are drawn from a Gaussian distribution with identity covariance matrix.

Generalized linear models. In binary classification under a generalized linear model, there is an increasing function $f : \mathbb{R} \rightarrow [0, 1]$, a.k.a. link function, along with a linear predictor $\beta \in \mathbb{R}^k$, where the score function $f(z^\top \beta)$ denotes the likelihood of feature vector z accepting the positive label. Formally, the data generating law for this classification problem under the low-dimensional manifold model of Section 2.2 can be formulated as the following:

$$y = \begin{cases} +1 & \text{w.p. } f(z^\top \beta), \\ -1 & \text{w.p. } 1 - f(z^\top \beta). \end{cases}, \quad x = \varphi(Wz), \quad z \sim \text{N}(0, I_k). \quad (5)$$

Popular choices of the link function f are the logistic model $f(t) = 1/(1 + \exp(-t))$, and the probit model $f(t) = \Phi(t)$ with $\Phi(t)$ being the standard normal cumulative distribution function.

2.4 Background on optimal classifiers

For each classification setup described in the previous section, we want to identify the classifiers that are optimal with respect to standard risk. To this end, we provide a summary of the Bayes-optimal classifiers. For a data point $(x, y) \sim \mathbb{P}_{x,y}$, consider the conditional distribution function $\eta(x) := \mathbb{P}(y = +1|X = x)$. This distribution function can be perceived as a likelihood of assigning the positive label to a data point with feature vector x . The Bayes-optimal classifier simply assigns label $y = +1$ to the feature vector x , if for this feature there is a higher likelihood to accept the label $+1$ than -1 . In other words, $h_{\text{Bayes}}(x) = \text{sign}(\eta(x) - 1/2)$. The next proposition states the optimality of the Bayes-optimal classifier.

Proposition 2.1. *Among all the classifiers $h : \mathbb{R}^d \rightarrow \{+1, -1\}$, such that h is a Borel function, the Bayes-optimal classifier $h_{\text{Bayes}}(x) = \text{sign}(\eta(x) - 1/2)$ has the lowest standard risk.*

Proof of Proposition 2.1 is provided in Section 4. The next corollary uses Proposition 2.1 to characterize the Bayes-optimal classifier under each of the binary classification settings described earlier in Section 2.3.

Corollary 2.2. *Under the Gaussian mixture model (4), the Bayes-optimal classifier can be formulated by*

$$h^*(x) = \text{sign} \left(\varphi^{-1}(x)^\top (WW^\top)^\dagger W\mu - q/2 \right),$$

with $q = \log(\frac{1-p}{p})$. Moreover, under the generalized linear model (5), the Bayes-optimal classifier is given by

$$h^*(x) = \text{sign} \left(f \left(\beta^\top (W^\top W)^{-1} W^\top \varphi^{-1}(x) \right) - 1/2 \right).$$

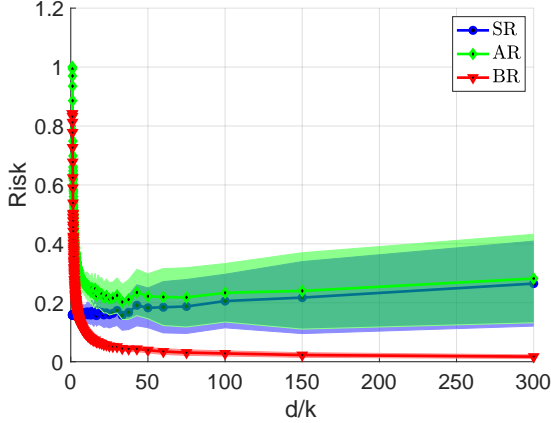
It is worth noting that in the described manifold latent model of Section 2.2, the weight matrix W is tall and full-rank, and φ is strictly increasing hence both $W^\top W$ and φ are invertible.

3 Main results

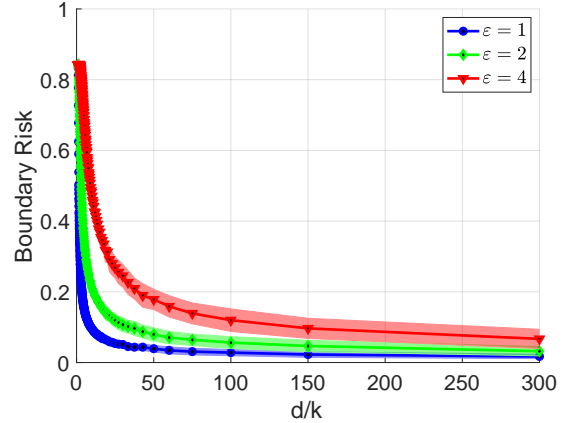
We will focus on the described binary classification settings of Section 2.3. In each setting, we will characterize the asymptotic behavior of the associated boundary risk of Bayes-optimal classifiers, when the ambient dimension d grows to infinity. Finally, we will validate our results through a set of synthetic numerical experiments.

3.1 Gaussian mixture model

In this section, we consider the Gaussian mixture model with features lying on a low-dimensional manifold. In this setting, data points are drawn from the generative rule (4). It is worth remembering that the learner only observes the ambient d -dimensional features x , and is oblivious to the original k -dimensional manifold features z . The next result states that under this setup, the boundary risk of the Bayes-optimal classifier will converge to zero, when the weight matrix W satisfies certain conditions.



(a) Behavior of the standard and adversarial risks of the Bayes-optimal classifier for the adversary’s power $\varepsilon = 1$.



(b) Behavior of the boundary risk of the Bayes-optimal classifier for the several values of adversary’s power ε .

Figure 1: Effect of the dimensions ratio d/k on the standard, adversarial, and the boundary risk of the Bayes-optimal classifier under the Gaussian mixture model (4), where features lie on a low-dimensional manifold. Solid curves represent the average values, and the shaded area around each curve represents one standard deviation above and below the computed average curve over the $M = 100$ realizations.

Theorem 3.1. *Consider the binary classification problem under the Gaussian mixture model (4). By letting the ambient dimension d grow to infinity, under the condition that the weight matrix W satisfies $\kappa(W)/\|W\|_F = o(1/\sqrt{k})$, the boundary risk of the Bayes-optimal classifier converges to zero.*

The proof of Theorem 3.1 is given in Section 4.3.

As a simple example that the conditions on the matrix W of Theorem 3.1 are satisfied, consider a matrix W that has equal non-zero singular values with unit norm rows. In this setup, if the dimensions ratio k/d converges to zero, then conditions of Theorem 3.1 are satisfied with $\kappa(W) = 1$, and $\|W\|_F^2 = d$.

Figure 1 validates the result of Theorem 3.1 under the Gaussian mixture model (4) with $p = 1/2$, and $\mu = \mathcal{N}(0, I_k/k)$. In this example, we fix the high-dimensional feature dimension $d = 300$, and vary the dimensions ratio d/k from 1 to 300. Further, we consider the identical function $\varphi(t) = t$, and let the feature matrix W have independent Gaussian entries $\mathcal{N}(0, 1/k)$. Figure 1a shows the effect of dimensions ratio d/k on the standard risk, adversarial risk, and the boundary risk of the Bayes-optimal classifier. For each fixed values (k, d) , we generate $M = 100$ independent realizations and compute the risks. The shaded area around each curve denotes one standard deviation (computed over M realizations) above and below the average curve. As it can be seen, the boundary risk will eventually converge to zero. Finally, in Figure 1b, we consider several values for adversary’s power, where it can be observed that for all adversary’s power ε , the boundary risk decays to zero as the feature dimensions d/k grows.

3.1.1 Does the boundary risk of all classifiers always vanish under the low-dimensional latent structure? An illustrative example

In Theorem (3.1), we showed that when features lie on a low-dimensional manifold, the Bayes optimal classifier is also optimal with respect to the adversarial risk. In the next proposition, we provide a simple example to show that such behavior (vanishing boundary risk) does not necessarily happen for all classifiers.

Proposition 3.2. *Consider the Gaussian mixture model (4) with μ having i.i.d. $N(0, 1)$ entries, and assume that the rows of the feature matrix W are sampled from the k -dimensional unit sphere $\mathbb{S}^{k-1}(1)$. Further, let φ be the identity function, and the sign probability $p = 1/2$. The boundary risk of the classifier $h(x) = \text{sign}(e_1^\top x)$ with $e_1 = (1, 0, 0, \dots, 0)$ is not smaller than some constant c_ε , where c_ε only depends on ε (independent of feature dimensions k, d), and it is strictly positive for positive values of ε .*

We refer to Section 4 for proof of this proposition.

3.2 Binary classification under generalized linear models

In this section, we consider binary classification under a generalized linear model with features having a low-dimensional latent structure. In this setting, data points are sampled from the data generative law (5). The next result states that under certain conditions on the linear predictor and the weight matrix, the boundary risk of the Bayes-optimal classifier will converge to zero.

Theorem 3.3. *Consider the binary classification problem under the generalized linear model (5). Assume that as the ambient dimension d grows to infinity, the weight matrix W satisfies the following condition:*

$$\kappa(W)/\|W\|_F = o\left(1/\sqrt{k}\right).$$

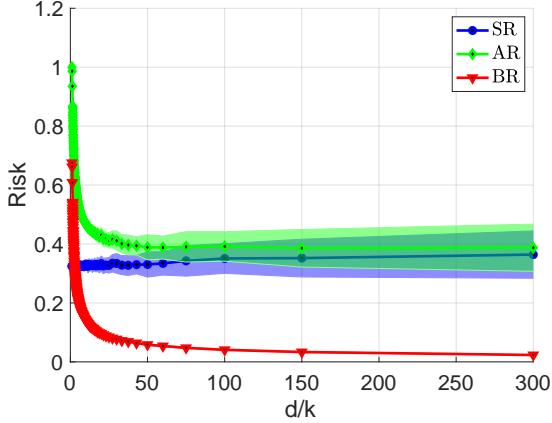
Then the boundary risk of the Bayes-optimal classifier will converge to zero.

The proof of Theorem 3.3 is given in Section 4.

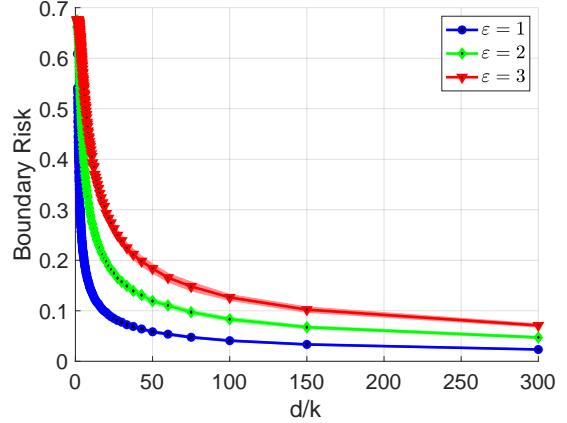
Figure 2 validates the result of Theorem 3.3 for binary classification under the generalized linear model (5) with identity φ mapping. In this example, the ambient dimension d is fixed at 300, and the manifold dimension k varies from 1 to 300. In addition, the linear predictor β and the weight matrix W have i.i.d. $N(0, 1/k)$ entries. For each fixed values (k, d) , we generate $M = 100$ independent realizations, and we compute the average and the standard deviation of total M obtained values. In each figure, the shaded areas are obtained by moving the average values one standard deviation above and below. Figure 2a denotes the behavior of the standard risk, adversarial risk, and the boundary risk of the Bayes-optimal classifier, as the dimensions ratio d/k grows. Further, Figure 2b exhibits a similar behavior for several values of adversary's power ε , in which it can be observed that the boundary risk will eventually decays to zero.

3.3 Is learning the latent structure necessary to have a vanishing boundary risk? A simple case

In the previous sections, for two binary classification settings, we showed that when features inherently have a low-dimensional structure, the boundary risk of the Bayes-optimal classifiers will



(a) Behavior of the standard and adversarial risks of the Bayes-optimal classifier for the adversary's power $\varepsilon = 1$.



(b) Behavior of the boundary risk of the Bayes-optimal classifier for the several values of adversary's power ε .

Figure 2: Effect of the dimensions ratio d/k on the standard, adversarial, and the boundary risk of the Bayes-optimal classifier of the generalized linear model (5), in which features are coming from a low-dimensional manifold. Solid curves represent the average values, and the shaded areas represent one standard deviation above and below the corresponding curves over $M = 100$ realizations.

converge to zero, as the ambient dimension grows to infinity. A closer look at the Bayes-optimal classifier of each setting (can be seen in Corollary 2.2) reveals the fact that these classifiers directly use the knowledge of the nonlinear mapping from the low-dimensional manifold to the ambient space. In other words, the Bayes-optimal classifiers explicitly draw upon the generative components φ and W . In this section, we investigate the existence of classifiers that are agnostic to the mapping between the low-dimensional and the high-dimensional space, while they have asymptotically vanishing boundary risk. For this purpose, consider binary classification under the Gaussian mixture model (4). In addition, assume that n samples $\{(x_i, y_i)\}_{i=1:n}$ are sampled from (4). We focus on the class of linear classifiers $h_\theta(x) = \text{sign}(x^\top \theta)$ with $\theta \in \mathbb{R}^d$. We consider the logistic loss $\ell(t) = \log(1 + \exp(-t))$, and assume that the adversary's power is bounded by ε . We consider the minimax approach of Madry et al. (2018b) to adversarially train a model θ by solving the following robust empirical risk minimization (ERM):

$$\hat{\theta}^\varepsilon = \arg \min_{\theta \in \mathbb{R}^d} \frac{1}{n} \sum_{i=1}^n \max_{u \in B_\varepsilon(x_i)} \ell(y_i u^\top \theta).$$

This is a convex optimization problem, as it can be cast as a point-wise maximization of the convex functions $\ell(y_i u^\top \theta)$. Further, when perturbations are from the ℓ_2 ball, the inner maximization problem can be solved explicitly (see e.g. Javanmard and Soltanolkotabi (2020)), which leads to the following equivalent problem:

$$\hat{\theta}^\varepsilon = \arg \min_{\theta \in \mathbb{R}^d} \frac{1}{n} \sum_{i=1}^n \ell(y_i x_i^\top \theta - \varepsilon \|\theta\|_{\ell_2}). \quad (6)$$

Figure 3 demonstrates the effect of the dimensions ratio d/k on the standard, adversarial, and the boundary risk of the classifier $h_{\hat{\theta}^\varepsilon}$ for four different choices of the feature mapping φ : (i) $\varphi_1(t) = t$,

(ii) $\varphi_2(t) = t/4 + \text{sign}(t)3t/4$, (iii) $\varphi_3(t) = t + \text{sign}(t)t^2$, and (iv) $\varphi_4(t) = \tanh(t)$. In this example, we consider the ambient dimension $d = 100$, and number of samples $n = 300$. In addition, k varies from 1 to 100, and μ, W have i.i.d. entries $\mathbf{N}(0, 1/k)$. Further, we consider balanced classes (each label ± 1 occurs with probability $p = 1/2$). The plots in Figure 3 exhibit the behavior of the standard, adversarial, and the boundary risks of the classifier $h_{\hat{\theta}^\varepsilon}$, for each of these mappings and for the adversary's power $\varepsilon = 1$. For each fixed value of k, d , we consider $M = 20$ trails of the setup. The solid curve denote the average values over these M trails. The shaded areas are obtained by plotting one standard deviation above and below the main curves. The plots in Figure 4 showcase the boundary risk for different choices of ε . As we observe, the boundary risk decreases to zero, when the dimensions ratio d/k grows to infinity. Our next theorem proves this behavior for the special case of $\varphi(t) = t$.

Theorem 3.4. *Consider binary classification under the Gaussian mixture model (4) with identity mapping $\varphi(t) = t$. Let $h_\theta(x) = \text{sign}(x^\top \theta)$ be a linear classifier with $\theta \in \mathbb{R}^d$ and assume that as the ambient dimension d grows to infinity, the following conditions on the weight matrix W and the decision parameter θ hold:*

$$\begin{aligned} \kappa(W)/\|W\|_F &= o\left(1/\sqrt{k}\right), \\ \left\|P_{\text{Ker}(W^\top)}(\theta)\right\|_{\ell_2} &= o\left(\|\theta\|_{\ell_2}\right), \end{aligned} \tag{7}$$

where $P_{\text{Ker}(W)}(\theta)$ stands for the ℓ_2 -projection of vector θ onto the kernel of the matrix W . Then the boundary risk of the classifier h_θ will converge to zero.

In particular, assume that $\hat{\theta}^\varepsilon$ is the solution of the following adversarial empirical risk minimization (ERM) problem:

$$\hat{\theta}^\varepsilon = \arg \min_{\theta \in \mathbb{R}^d} \frac{1}{n} \sum_{i=1}^n \sup_{u \in B_\varepsilon(x_i)} \ell(y_i u^\top \theta),$$

with $\ell : \mathbb{R} \rightarrow \mathbb{R}^{\geq 0}$ being a strictly decreasing loss function. In this case, with the weight matrix W satisfying $\kappa(W)/\|W\|_F = o(1/\sqrt{k})$, the boundary risk of $h_{\hat{\theta}^\varepsilon}$ will converge to zero.

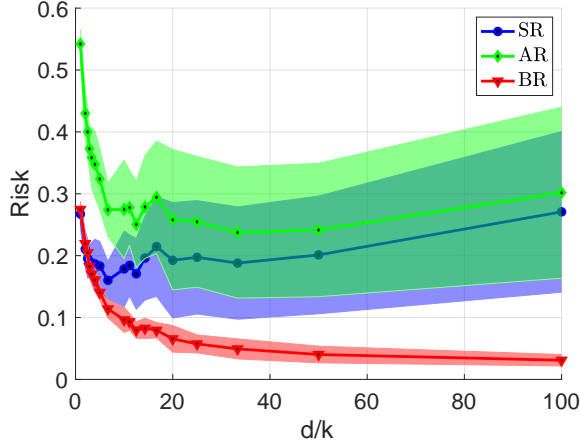
Proof of Theorem 3.4 is deferred to Section 4.6.

4 Proof of theorems and technical lemmas

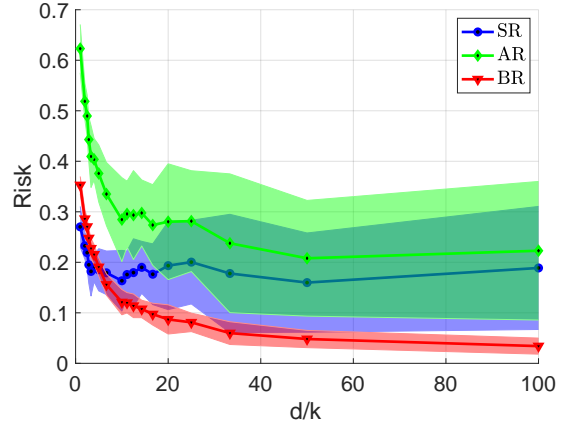
4.1 Proof of Proposition 2.1

Denote the Bayes-optimal classifier by $h^*(x) := \text{sign}(\eta(x) - 1/2)$. Consider a classifier h where the set $A = \{x : h(x) = +1\}$ is Borel measurable. We denote the complement of A with $A^c = \mathbb{R}^d \setminus A$. Our goal is to show that $\text{SR}(h^*) \leq \text{SR}(h)$. First, for every $x \in \mathbb{R}^d$, and a Borel measurable set B , it is easy to check that the following holds:

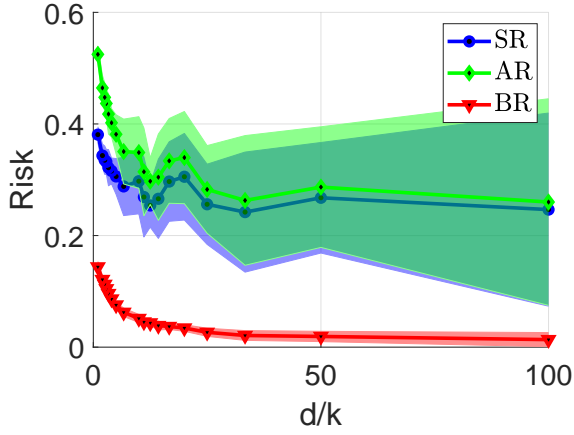
$$(2\eta(x) - 1) \cdot (\mathbb{I}(x \in B) - \mathbb{I}(\eta(x) \leq 1/2)) \geq 0. \tag{8}$$



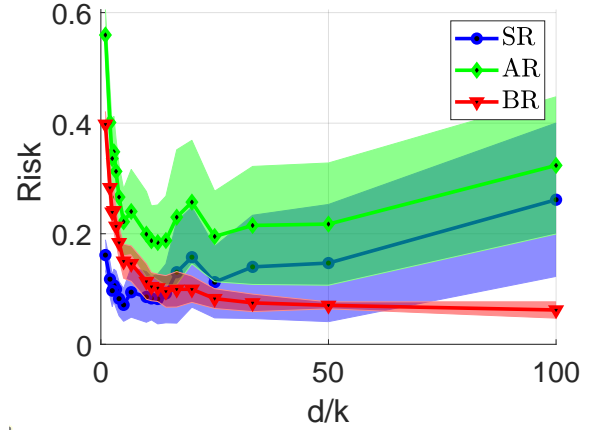
(a) Feature mapping $\varphi(t) = t$ and adversary's power $\varepsilon = 1$



(b) Feature mapping $\varphi(t) = t/4 + \text{sign}(t)3t/4$ and adversary's power $\varepsilon = 1$

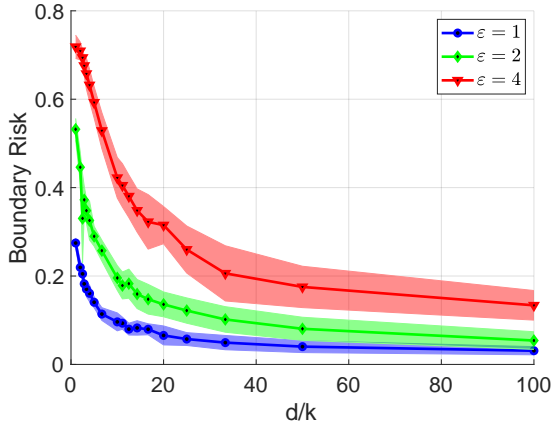


(c) Feature mapping $\varphi(t) = t + \text{sign}(t)t^2$ and adversary's power $\varepsilon = 1$

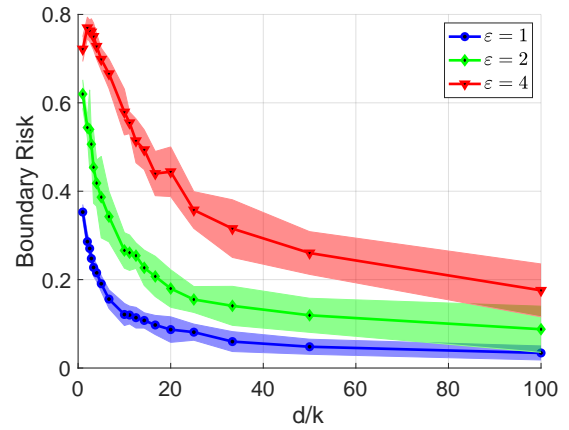


(d) Feature mapping $\varphi(t) = \tanh(t)$ and adversary's power $\varepsilon = 1$.

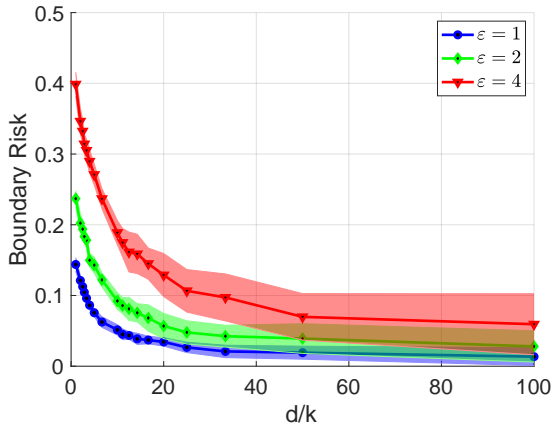
Figure 3: Effect of dimensions ratio d/k on the standard, adversarial, and boundary risks of the linear classifier $h_\theta(x) = \text{sign}(x^\top \theta)$ with θ being the robust empirical risk minimizer (6). Samples are generated from the Gaussian mixture model (4) with balanced classes ($p = 1/2$), and with four choices of feature mapping φ : (a) $\varphi(t) = t$, (b) $\varphi(t) = 3t/4 + \text{sign}(t)t/4$, (c) $\varphi(t) = t + \text{sign}(t)t^2$ and (d) $\varphi(t) = \tanh(t)$. In these experiments, the ambient dimension d is fixed at 100, and the manifold dimension k varies from 1 to 100. The sample size is $n = 300$ the classes average μ and the weight matrix W have i.i.d. entries from $N(0, 1/k)$. The adversary's power is fixed at $\varepsilon = 1$. For each fixed values of k and d , we consider $M = 20$ trails of the setup. Solid curves represent the average results across these trials, and the shaded areas represent one standard deviation above and below the corresponding curves.



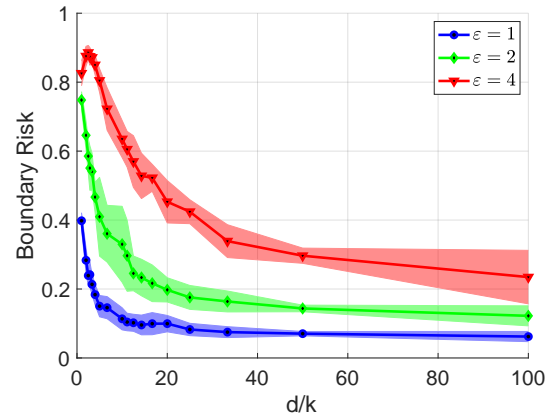
(a) Boundary risk with the feature mapping $\varphi(t) = t$ and for multiple values of adversary's power ε



(b) Boundary risk with the feature mapping $\varphi(t) = t/4 + \text{sign}(t)3t/4$ and for multiple values of adversary's power ε



(c) Boundary risk with the feature mapping $\varphi(t) = t + \text{sign}(t)t^2$ and for multiple values of adversary's power ε



(d) Boundary risk with the feature mapping $\varphi(t) = \tanh(t)$ and for multiple values of adversary's power ε

Figure 4: Effect of dimensions ratio d/k on the boundary risk of the linear classifier $h_\theta(x) = \text{sign}(x^\top \theta)$ with θ being the robust empirical risk minimizer (6). Samples are generated from the Gaussian mixture model (4) with balanced classes ($p = 1/2$), and with four choices of feature mapping φ : (a) $\varphi(t) = t$, (b) $\varphi(t) = 3t/4 + \text{sign}(t)t/4$, (c) $\varphi(t) = t + \text{sign}(t)t^2$ and (d) $\varphi(t) = \tanh(t)$. In these experiments, the ambient dimension d is fixed at 100, and the manifold dimension k varies from 1 to 100. The sample size is $n = 300$ the classes average μ and the weight matrix W have i.i.d. entries from $N(0, 1/k)$. We consider different levels of the adversary's power $\varepsilon \in \{1, 2, 4\}$. For each fixed values of k and d , we consider $M = 20$ trials of the setup. Solid curves represent the average results across these trials, and the shaded areas represent one standard deviation above and below the corresponding curves.

On the other hand, we have

$$\begin{aligned}
\text{SR}(h) &= \mathbb{P}(h(x)y \leq 0) \\
&= \mathbb{E}[\mathbb{I}(x \in A^c, y = +1) + \mathbb{I}(x \in A, y = -1)] \\
&= \mathbb{E}_x [\mathbb{E}[\mathbb{I}(x \in A^c, y = +1) + \mathbb{I}(x \in A, y = -1)|x]] \\
&= \mathbb{E}_x [\mathbb{I}(x \in A^c)\eta(x) + \mathbb{I}(x \in A)(1 - \eta(x))] .
\end{aligned}$$

By using the identity $\mathbb{I}(x \in A) + \mathbb{I}(x \in A^c) = 1$, we can simplify the above equation to arrive at the following:

$$\text{SR}(h) = \mathbb{E}_x [\mathbb{I}(x \in A^c)(2\eta(x) - 1) + 1 - \eta(x)] . \quad (9)$$

Note that the above equation holds for all classifiers h . In particular, we can employ it for h^* . For this purpose, we know that the subset of \mathbb{R}^d with the negative label is $A^{*c} = \{x : \eta(x) \leq 1/2\}$. By recalling (9) for h^* we get:

$$\text{SR}(h^*) = \mathbb{E}_x [\mathbb{I}(\eta(x) \leq 1/2)(2\eta(x) - 1) + 1 - \eta(x)] . \quad (10)$$

We can subtract (10) from (9), and then exploit (8) with substituting B with A^c to get $\text{SR}(h) \geq \text{SR}(h^*)$. This completes the proof.

4.2 Proof of Corollary 2.2

In order to characterize the Bayes-optimal classifier of the Gaussian mixture setting (4), we first need to compute the conditional density function $\mathbb{P}(y = +1|x)$. This will help us use Proposition 2.1 to identify the Bayes-optimal classifiers. For this purpose, in the first step, consider the general Gaussian mixture model $\tilde{x} \sim \mathbf{N}(y\tilde{\mu}, \Sigma)$, where the covariance matrix Σ is not necessarily full-rank. This means that \tilde{x} can be a degenerate multivariate Gaussian with the following density function:

$$f_{\tilde{x}|y}(\tilde{x}) = (|2\pi\Sigma|_+)^{-1/2} \exp\left(-(\tilde{x} - y\tilde{\mu})^\top \Sigma^\dagger (\tilde{x} - y\tilde{\mu})/2\right) , \quad (11)$$

where $|\cdot|_+$ stands for the pseudo-determinant operator. By recalling the Bayes' theorem we get

$$\begin{aligned}
\mathbb{P}(y = +1|\tilde{x}) &= \frac{\mathbb{P}(y = +1)f_{\tilde{x}|y=+1}(\tilde{x})}{\mathbb{P}(y = +1)f_{\tilde{x}|y}(\tilde{x}) + \mathbb{P}(y = -1)f_{\tilde{x}|y=-1}(\tilde{x})} \\
&= \frac{1}{1 + ((1-p)/p) \cdot f_{\tilde{x}|y=-1}(\tilde{x})/f_{\tilde{x}|y=+1}(\tilde{x})} .
\end{aligned}$$

By using (11) in the last equation, we will arrive at the following

$$\mathbb{P}(y = +1|\tilde{x}) = \left(1 + \exp(-2\tilde{x}^\top \Sigma^\dagger \tilde{\mu} + q)\right)^{-1} , \quad (12)$$

where $q = \log \frac{1-p}{p}$. On the other hand, it is easy to observe that

$$\text{sign}((1 + \exp(-t))^{-1} - 1/2) = \text{sign}(t) . \quad (13)$$

Finally, we can deploy (12) in Proposition 2.1 in conjunction with the identity (13) to derive the Bayes-optimal classifier $\tilde{h}^* = \text{sign}(\tilde{x}^\top \Sigma^\dagger \tilde{\mu} - q/2)$. We can now focus on the primary setup (4). Let $\Sigma := WW^\top$, $\tilde{x} = \varphi^{-1}(x)$, and $\tilde{\mu} := W\mu$. It is easy to check that with these new notations we have $\tilde{x} \sim \mathbf{N}(y\tilde{\mu}, \Sigma)$. Recall the Bayes-optimal classifier of this setting $h^*(x) = \text{sign}(\tilde{x}^\top \Sigma^\dagger \tilde{\mu} - q/2)$. By replacing \tilde{x} , Σ , and $\tilde{\mu}$ by their respective definitions $\varphi^{-1}(x)$, WW^\top , and $W\mu$ we realize that the Bayes-optimal classifier is given by

$$h^*(x) = \text{sign} \left(\varphi^{-1}(x)^\top (WW^\top)^\dagger W\mu - q/2 \right).$$

In this part we want to characterize the Bayes-optimal classifier of the generalized linear model (5). To this end, note that if the proposed classifier in Corollary 2.2 is optimal for the identity map $\varphi(x) = x$, then we can simply consider $\tilde{x} = \varphi^{-1}(x)$, and establish its optimality for every function φ . This means that we can only focus on the case with the identity function $\varphi(x) = x$. For the purpose of identifying the Bayes-optimal classifiers, we can use Proposition 2.1. In the first step, we need to compute the conditional probability $\mathbb{P}(y = 1|x)$. By using the Bayes rule we get

$$\begin{aligned} \mathbb{P}(y = +1|X = x) &= \frac{\int \mathbb{P}_{X|Z}(x|z) \mathbb{P}_{Y|X,Z}(+1|x, z) d\mathbb{P}_Z(z)}{\int \mathbb{P}_{X|Z}(x|z) d\mathbb{P}_Z(z)} \\ &= \frac{\int \mathbb{I}(Wz = x) \mathbb{P}_{Y|Z}(+1|z) d\mathbb{P}_Z(z)}{\int \mathbb{I}(Wz = x) d\mathbb{P}_Z(z)}, \end{aligned}$$

where in the last equation, we used the fact that condition on z , the feature vector x and the label y are independent. In addition, as W is a full-rank matrix (linearly independent columns), then for a fixed x , equation $Wz = x$ has the unique solution $z^* = (W^\top W)^{-1} W^\top x$. This gives us

$$\begin{aligned} \mathbb{P}(y = +1|X = x) &= \mathbb{P}_{Y|Z}(+1|z^*) \\ &= f(\beta^\top (W^\top W)^{-1} W^\top x). \end{aligned}$$

By recalling Proposition 2.1, we realize that the Bayes-optimal classifier of this setting with $\varphi(t) = t$ is given by

$$h^*(x) = \text{sign} \left(f(\beta^\top (W^\top W)^{-1} W^\top x) - 1/2 \right).$$

This completes the proof.

4.3 Proof of Theorem 3.1

Introduce $\rho(\cdot) = \varphi^{-1}(\cdot)$, $\Sigma = WW^\top$, $\tilde{x} = \rho(x)$, and $\tilde{\mu} = W\mu$. From Corollary 2.2, we know that the Bayes-optimal classifier is given by

$$h^*(x) = \text{sign} \left(\rho(x)^\top (WW^\top)^\dagger W\mu - q/2 \right). \quad (14)$$

We next focus on computing the boundary risk of the Bayes-optimal classifier h^* . By recalling the boundary risk definition we get:

$$\text{BR}(h^*) = \mathbb{P}_{x,y} \left(h^*(x)y \geq 0, \inf_{u \in B_\varepsilon(x)} h^*(x)h^*(u) \leq 0 \right).$$

In the next step, we expand the above expression for the two possible values of $y \in \{+1, -1\}$ to get

$$\begin{aligned} \text{BR}(h^*) &= \mathbb{P}_{x,y} \left(h^*(x) \geq 0, \inf_{u \in B_\varepsilon(x)} h^*(u) \leq 0, y = 1 \right) \\ &\quad + \mathbb{P}_{x,y} \left(h^*(x) \leq 0, \sup_{u \in B_\varepsilon(x)} h^*(u) \geq 0, y = -1 \right). \end{aligned}$$

We then plug (14) into the last equation to get

$$\begin{aligned} \text{BR}(h^*) &\leq \mathbb{P}_{x,y} \left(\inf_{u \in B_\varepsilon(x)} \tilde{\mu}^\top \Sigma^\dagger \rho(u) \leq \frac{q}{2} \leq \tilde{x}^\top \Sigma^\dagger \tilde{\mu}, y = 1 \right) \\ &\quad + \mathbb{P}_{x,y} \left(\tilde{x}^\top \Sigma^\dagger \tilde{\mu} \leq \frac{q}{2} \leq \sup_{u \in B_\varepsilon(x)} \tilde{\mu}^\top \Sigma^\dagger \rho(u), y = -1 \right). \end{aligned}$$

By our assumption, $d\varphi/dt \geq c$, for some constant $c > 0$. By simple algebraic manipulation it is easy to check that $\rho(B_\varepsilon(x))$ is a subset of $B_{\varepsilon/c}(\rho(x))$. This gives us

$$\begin{aligned} \text{BR}(h^*) &\leq \mathbb{P}_{x,y} \left(\inf_{v \in B_{\varepsilon/c}(\tilde{x})} \tilde{\mu}^\top \Sigma^\dagger v \leq \frac{q}{2} \leq \tilde{x}^\top \Sigma^\dagger \tilde{\mu}, y = +1 \right) \\ &\quad + \mathbb{P}_{x,y} \left(\tilde{x}^\top \Sigma^\dagger \tilde{\mu} \leq \frac{q}{2} \leq \sup_{v \in B_{\varepsilon/c}(\tilde{x})} \tilde{\mu}^\top \Sigma^\dagger v, y = -1 \right). \end{aligned}$$

The inner minimization in the above expression can be solved in closed form, by which we obtain

$$\begin{aligned} \text{BR}(h^*) &\leq \mathbb{P}_{x,y} \left(\frac{q}{2} \leq \tilde{x}^\top \Sigma^\dagger \tilde{\mu} \leq \frac{q}{2} + \frac{\varepsilon}{c} \left\| \Sigma^\dagger \tilde{\mu} \right\|_{\ell_2}, y = 1 \right) \\ &\quad + \mathbb{P}_{x,y} \left(\frac{q}{2} - \frac{\varepsilon}{c} \left\| \Sigma^\dagger \tilde{\mu} \right\|_{\ell_2} \leq \tilde{x}^\top \Sigma^\dagger \tilde{\mu} \leq \frac{q}{2}, y = -1 \right). \end{aligned}$$

From the Gaussian mixture model (4) we know that $x \sim \mathbf{N}(y\tilde{\mu}, \Sigma)$. For $\tilde{x}_+ \sim \mathbf{N}(\tilde{\mu}, \Sigma)$ and $\tilde{x}_- \sim \mathbf{N}(-\tilde{\mu}, \Sigma)$ this implies that $\tilde{x}|y = +1 \sim \tilde{x}_+$, and $\tilde{x}|y = -1 \sim \tilde{x}_-$. By conditioning the above expression on y we get:

$$\begin{aligned} \text{BR}(h^*) &\leq p \mathbb{P}_{\tilde{x}_+} \left(0 \leq \tilde{x}_+^\top \Sigma^\dagger \tilde{\mu} - \frac{q}{2} \leq \varepsilon \left\| \Sigma^\dagger \tilde{\mu} \right\| / c \right) \\ &\quad + (1-p) \mathbb{P}_{\tilde{x}_-} \left(-\frac{\varepsilon}{c} \left\| \Sigma^\dagger \tilde{\mu} \right\| \leq \tilde{x}_-^\top \Sigma^\dagger \tilde{\mu} - \frac{q}{2} \leq 0 \right). \end{aligned}$$

Since $\tilde{x}_+^\top \Sigma^\dagger \tilde{\mu} \sim \mathbf{N}(a, a)$, and $\tilde{x}_-^\top \Sigma^\dagger \tilde{\mu} \sim \mathbf{N}(-a, a)$ with $a = \tilde{\mu}^\top \Sigma^\dagger \tilde{\mu}$, we have

$$\begin{aligned} \text{BR}(h^*) &\leq p \mathbb{P}_{u \sim \mathbf{N}(a,a)} \left(0 \leq u - \frac{q}{2} \leq \frac{\varepsilon}{c} \left\| \Sigma^\dagger \tilde{\mu} \right\| \right) \\ &\quad + (1-p) \mathbb{P}_{u \sim \mathbf{N}(-a,a)} \left(-\frac{\varepsilon}{c} \left\| \Sigma^\dagger \tilde{\mu} \right\| \leq u - \frac{q}{2} \leq 0 \right). \end{aligned}$$

We bound the above probabilities, using that the pdf of normal $\mathbf{N}(\nu, \sigma)$ is bounded by $1/\sqrt{2\pi\sigma}$, for any values of $\sigma > 0$ and ν . This implies that

$$\text{BR}(h^*) \leq \frac{\varepsilon \left\| \Sigma^\dagger \tilde{\mu} \right\|}{c \sqrt{2\pi} \left\| \Sigma^\dagger \tilde{\mu} \right\|}. \quad (15)$$

Consider a singular value decomposition $W = USV^\top$. Then, $\Sigma^\dagger = US^{-2}U^\top$, and $\tilde{\mu} = USV^\top\mu$. Pluggin these relations into (15) we get

$$\frac{\sqrt{2\pi}c\text{BR}(h^*)}{\varepsilon} \leq \frac{\|US^{-1}V^\top\mu\|}{\|UV^\top\mu\|} = \frac{\|S^{-1}V^\top\mu\|}{\|V^\top\mu\|} \leq \|S^{-1}\|, \quad (16)$$

where we used that $U^\top U = I$. By recalling the definition of the condition number $\kappa(W) = \|W\| \|W^\dagger\|$, we get

$$\|S^{-1}\| = \kappa(W)/\|W\| \leq \sqrt{k} \cdot \kappa(W)/\|W\|_F. \quad (17)$$

The claim follows by combining (16) and (17).

4.4 Proof of Proposition 3.2

From the definition of boundary risk in (3) we have

$$\text{BR}(h) = \mathbb{P} \left(h(x)y \geq 0, \inf_{x' \in B_\varepsilon(x)} h(x')h(x) \leq 0 \right).$$

Note that the above probability involves the randomness of $\mu \sim \mathbf{N}(0, I_k)$, and entries of W being $\mathbf{N}(0, 1/k)$. In the first step, for the classifier $h(x) = \text{sign}(x^\top e_1)$, expand the boundary risk for each possible values of $y \in \{+1, -1\}$ to get

$$\begin{aligned} \text{BR}(h) &= \mathbb{P} \left(x^\top e_1 \geq 0, \inf_{x' \in B_\varepsilon(x)} \text{sign}(x'^\top e_1) \leq 0, y = +1 \right) + \\ &\quad \mathbb{P} \left(x^\top e_1 \leq 0, \sup_{x' \in B_\varepsilon(x)} \text{sign}(x'^\top e_1) \geq 0, y = -1 \right). \end{aligned}$$

We next solve the inner optimizations over the ℓ_2 ball with ε radius to get

$$\begin{aligned} \text{BR}(h) &= \mathbb{P} \left(0 \leq x^\top e_1 \leq \varepsilon, y = +1 \right) + \\ &\quad \mathbb{P} \left(-\varepsilon \leq x^\top e_1 \leq 0, y = -1 \right). \end{aligned}$$

Note that in the setting (4), $\varphi(t) = t$ hence we have $x|y \sim \mathbf{N}(yW\mu, WW^\top)$. By conditioning on the W, μ we get

$$\begin{aligned} \text{BR}(h) &= p \cdot \mathbb{E}_{W, \mu} \left[\mathbb{P}_{x \sim \mathbf{N}(W\mu, WW^\top)} \left(0 \leq x^\top e_1 \leq \varepsilon \right) \right] + \\ &\quad (1 - p) \cdot \mathbb{E}_{W, \mu} \left[\mathbb{P}_{x \sim \mathbf{N}(-W\mu, WW^\top)} \left(-\varepsilon \leq x^\top e_1 \leq 0 \right) \right]. \end{aligned}$$

We next denote the first column of W^\top by $\omega \in \mathbb{R}^k$. It is easy to observe that conditioned on μ and ω , the linear term $x^\top e_1$ has a Gaussian distribution with the mean $\mu^\top \omega$, and the unit variance (recall that ω lies on the unit k dimensional sphere). This brings us

$$\begin{aligned} \text{BR}(h) &= p \cdot \mathbb{E}_{\mu, \omega} \left[\mathbb{P}_{u \sim \mathbf{N}(\mu^\top \omega, 1)} (0 \leq u \leq \varepsilon) \right] + \\ &\quad (1 - p) \cdot \mathbb{E}_{\mu, \omega} \left[\mathbb{P}_{u \sim \mathbf{N}(-\mu^\top \omega, 1)} (-\varepsilon \leq u \leq 0) \right]. \end{aligned}$$

We then use the standard normal c.d.f. Φ to rewrite the above probabilities. This gives us the following:

$$\begin{aligned} \text{BR}(h) &= p \cdot \mathbb{E}_{\mu, \omega} \left[\Phi(\varepsilon - \mu^\top \omega) - \Phi(-\mu^\top \omega) \right] + \\ &\quad (1-p) \cdot \mathbb{E}_{\mu, \omega} \left[\Phi(\mu^\top \omega) - \Phi(-\varepsilon + \mu^\top \omega) \right] \\ &= \mathbb{E}_{\mu, \omega} \left[\Phi(\varepsilon - \mu^\top \omega) - \Phi(-\mu^\top \omega) \right], \end{aligned}$$

where the last equation comes from the fact that $\Phi(t) + \Phi(-t) = 1$, for every real value t . Next, note that condition on ω , the expression $\mu^\top \omega$ has standard normal distribution, as μ has i.i.d. standard normal entries. More precisely, by using the law of iterated expectations, we have:

$$\begin{aligned} \text{BR}(h) &= \mathbb{E}_{\mu, \omega} \left[\Phi(\varepsilon - \mu^\top \omega) - \Phi(-\mu^\top \omega) \right] \\ &= \mathbb{E}_{\omega} \left[\mathbb{E} \left[\Phi(\varepsilon - \mu^\top \omega) - \Phi(-\mu^\top \omega) \mid \omega \right] \right] \\ &= \mathbb{E}_{\omega} \left[\mathbb{E}_{Z \sim \mathcal{N}(0,1)} [\Phi(\varepsilon + Z) - \Phi(Z)] \right] = c_\varepsilon, \end{aligned}$$

with $c_\varepsilon = \mathbb{E}_{Z \sim \mathcal{N}(0,1)} [\Phi(\varepsilon + Z) - \Phi(Z)]$, which is a deterministic value independent of dimensions k, d .

4.5 Proof of Theorem 3.3

From Corollary 2.2, we know that the Bayes optimal classifier in this setting is given by

$$h^*(x) = \text{sign} \left(f(\beta^\top \widetilde{W}^\top \tilde{x}) - 1/2 \right), \quad (18)$$

where $\widetilde{W} = W(W^\top W)^{-1}$, and $\tilde{x} = \varphi^{-1}(x)$. We focus on computing the boundary risk of the optimal classifier h^* . In the first step, from the definition of the boundary risk we have

$$\text{BR}(h^*) = \mathbb{P} \left(h^*(x)y \geq 0, \inf_{u \in B_\varepsilon(x)} h^*(x)h^*(u) \leq 0 \right).$$

By conditioning on the value of y we get

$$\begin{aligned} \text{BR}(h^*) &= \mathbb{P} \left(y = +1, h^*(x) \geq 0, \inf_{u \in B_\varepsilon(x)} h^*(u) \leq 0 \right) + \\ &\quad \mathbb{P} \left(y = -1, h^*(x) \leq 0, \sup_{u \in B_\varepsilon(x)} h^*(u) \geq 0 \right). \end{aligned}$$

By removing conditions $y = +1$ and $y = -1$, we can upper bound the above probabilities. This gives us

$$\begin{aligned} \text{BR}(h^*) &\leq \mathbb{P} \left(h^*(x) \geq 0, \inf_{u \in B_\varepsilon(x)} h^*(u) \leq 0 \right) + \\ &\quad \mathbb{P} \left(h^*(x) \leq 0, \sup_{u \in B_\varepsilon(x)} h^*(u) \geq 0 \right). \end{aligned}$$

Plug (18) into the above expression to get

$$\begin{aligned} \text{BR}(h^*) &\leq \mathbb{P} \left(\inf_{u \in B_\varepsilon(x)} f \left(\varphi^{-1}(u)^\top \widetilde{W} \beta \right) \leq 1/2 \leq f(\tilde{x}^\top \widetilde{W} \beta) \right) + \\ &\quad \mathbb{P} \left(f(\tilde{x}^\top \widetilde{W} \beta) \leq 1/2 \leq \sup_{u \in B_\varepsilon(x)} f \left(\varphi^{-1}(u)^\top \widetilde{W} \beta \right) \right). \end{aligned}$$

From the manifold model of Section 2.2, we know that function φ is strictly increasing. This implies that there exists $c > 0$ such that its derivative $d\varphi/dt \geq c$. By simple algebraic computation along with the lower bound on the derivative of φ , it is easy to observe that $\varphi^{-1}(B_\varepsilon(x))$ is a subset of $B_{\varepsilon/c}(\varphi^{-1}(x))$. This yields

$$\begin{aligned} \text{BR}(h^*) &\leq \mathbb{P} \left(\inf_{v \in B_{\varepsilon/c}(\tilde{x})} f \left(v^\top \widetilde{W} \beta \right) \leq 1/2 \leq f(\tilde{x}^\top \widetilde{W} \beta) \right) + \\ &\quad \mathbb{P} \left(f(\tilde{x}^\top \widetilde{W} \beta) \leq 1/2 \leq \sup_{v \in B_{\varepsilon/c}(\tilde{x})} f \left(v^\top \widetilde{W} \beta \right) \right). \end{aligned}$$

Note that f is an increasing function, and the above inner optimizations can be seen as linear objectives over a bounded ℓ_2 -ball hence they have explicit solutions. We introduce $c_0 = f^{-1}(1/2)$ and rewrite the above equation as

$$\begin{aligned} \text{BR}(h^*) &\leq \mathbb{P} \left(c_0 \leq \tilde{x}^\top \widetilde{W} \beta \leq c_0 + \varepsilon \left\| \widetilde{W} \beta \right\|_{\ell_2} / c \right) + \\ &\quad \mathbb{P} \left(c_0 - \varepsilon \left\| \widetilde{W} \beta \right\|_{\ell_2} / c \leq \tilde{x}^\top \widetilde{W} \beta \leq c_0 \right). \end{aligned} \tag{19}$$

From the manifold latent model described in Section 2.2, we know that $\tilde{x} \sim \mathcal{N}(0, WW^\top)$. This implies that $\tilde{x}^\top \widetilde{W} \beta \sim \mathcal{N}(0, \|\beta\|_{\ell_2}^2)$, and the probability terms in (19) can be written in terms of the standard normal c.d.f. Φ . Let $\gamma = \widetilde{W} \beta$, we have

$$\text{BR}(h^*)/2 \leq \Phi \left(\frac{c_0 + \varepsilon \|\gamma\|_{\ell_2} / c}{\|\beta\|_{\ell_2}} \right) - \Phi \left(\frac{c_0 - \varepsilon \|\gamma\|_{\ell_2} / c}{\|\beta\|_{\ell_2}} \right).$$

By using the fact that Φ is $1/\sqrt{2\pi}$ -Lipschitz continuous, we get

$$\text{BR}(h^*) \leq \frac{4\varepsilon \left\| \widetilde{W} \beta \right\|_{\ell_2}}{c\sqrt{2\pi} \|\beta\|_{\ell_2}}. \tag{20}$$

We can write the SVD of the weight matrix W to get $W = USV^\top$. In this decomposition, matrices $U \in \mathbb{R}^{d \times k}$, $V \in \mathbb{R}^{k \times k}$ are semi-unitary, i.e. $U^\top U = V^\top V = I_k$, and the matrix $S \in \mathbb{R}^{k \times k}$ is diagonal with non-zero entries on its diagonal. Therefore $\widetilde{W} := W(W^\top W)^{-1} = US^{-1}V^\top$. By plugging this decomposition into (20), we get

$$\text{BR}(h^*) \leq \frac{4\varepsilon \left\| US^{-1}V^\top \beta \right\|_{\ell_2}}{c\sqrt{2\pi} \|\beta\|_{\ell_2}} = \frac{4\varepsilon \left\| S^{-1}V^\top \beta \right\|_{\ell_2}}{c\sqrt{2\pi} \|\beta\|_{\ell_2}}, \tag{21}$$

where the last equation comes from the fact that $U^\top U = I_k$.

In the last step, we consider the adjoint-kernel decomposition of the matrix W . In this decomposition, vector β can be written as $\beta = W^\top \alpha + \eta$, where $W\eta = 0$, and $\alpha \in \mathbb{R}^d$. Note that as $W\eta = 0$, it means that $V^\top \eta = 0$ hence $V^\top \beta = SU^\top \alpha$. By using this relation in (21) we get the following

$$c \cdot \text{BR}(h^*)/(2\varepsilon) \leq \frac{\|U^\top \alpha\|_{\ell_2}}{\|\beta\|_{\ell_2}}. \quad (22)$$

We can write $\|\beta\|_{\ell_2}^2 = \|W^\top \alpha\|_{\ell_2}^2 + \|\eta\|_{\ell_2}^2$, and combine this relation with $W = USV^\top$ to get

$$\|\beta\|_{\ell_2}^2 = \|SU^\top \alpha\|_{\ell_2}^2 + \|\eta\|_{\ell_2}^2.$$

This implies that $\|\beta\|_{\ell_2} \geq \|SU^\top \alpha\|_{\ell_2}$. By using this relation in (22) we arrive at

$$c \cdot \text{BR}(h^*)/(2\varepsilon) \leq \frac{\|U^\top \alpha\|_{\ell_2}}{\|SU^\top \alpha\|_{\ell_2}} \leq \frac{1}{\sigma_{\min}(S)}. \quad (23)$$

By recalling the condition number definition $\kappa(W) = \|W\| \|W^\dagger\|$, we get

$$1/\sigma_{\min}(S) = \kappa(W)/\sigma_{\max}(S) \leq \sqrt{k} \cdot \kappa(W)/\|W\|_F = o(1),$$

where in the last relation we used the fact that $\kappa(W)/\|W\|_F = o(1/\sqrt{k})$. Deploying $1/\sigma_{\min}(S) = o(1)$ in (23) completes the proof.

4.6 Proof of Theorem 3.4

By recalling the definition of the boundary risk we get

$$\text{BR}(h_\theta) = \mathbb{P}(h_\theta(x)y \geq 0, \inf_{x' \in B_\varepsilon(x)} h_\theta(x')h_\theta(x) \leq 0).$$

We expand the above probabilities with respect to the y possible values $\{+1, -1\}$. This gives us

$$\begin{aligned} \text{BR}(h_\theta) &= \mathbb{P}(y = +1, h_\theta(x) \geq 0, \inf_{x' \in B_\varepsilon(x)} h_\theta(x') \leq 0) + \\ &\quad \mathbb{P}(y = -1, h_\theta(x) \leq 0, \sup_{x' \in B_\varepsilon(x)} h_\theta(x') \geq 0). \end{aligned}$$

Plugging $h_\theta(x) = \text{sign}(x^\top \theta)$ into to the above expression yields

$$\begin{aligned} \text{BR}(h_\theta) &= \mathbb{P}(y = +1, x^\top \theta \geq 0, \inf_{x' \in B_\varepsilon(x)} \theta^\top x' \leq 0) + \\ &\quad \mathbb{P}(y = -1, x^\top \theta \leq 0, \sup_{x' \in B_\varepsilon(x)} \theta^\top x' \geq 0). \end{aligned}$$

By solving the inner optimizations we can get the following

$$\begin{aligned} \text{BR}(h_\theta) &= \mathbb{P}(y = +1, 0 \leq x^\top \theta \leq \varepsilon \|\theta\|_{\ell_2}) + \\ &\quad \mathbb{P}(y = -1, -\varepsilon \|\theta\|_{\ell_2} \leq x^\top \theta \leq 0). \end{aligned}$$

From the Gaussian mixture model (4) we know that $x|y \sim \mathbf{N}(yW\mu, WW^\top)$. By using this Gaussian distribution along with conditioning on values of y , we get

$$\begin{aligned} \text{BR}(h_\theta) &= p \cdot \mathbb{P}_{x \sim \mathbf{N}(W\mu, WW^\top)}(0 \leq x^\top \theta \leq \varepsilon \|\theta\|_{\ell_2}) + \\ &\quad (1-p) \cdot \mathbb{P}_{x \sim \mathbf{N}(-W\mu, WW^\top)}(-\varepsilon \|\theta\|_{\ell_2} \leq x^\top \theta \leq 0). \end{aligned}$$

As x has multivariate Gaussian distribution, we can rewrite the above probabilities in terms of the standard normal cdf Φ . Further, by using the identity $\Phi(t) + \Phi(-t) = 1$, we get

$$\text{BR}(h_\theta) = \Phi\left(\frac{\varepsilon \|\theta\|_{\ell_2} - \theta^\top W\mu}{\|W^\top \theta\|_{\ell_2}}\right) - \Phi\left(\frac{-\theta^\top W\mu}{\|W^\top \theta\|_{\ell_2}}\right).$$

The $1/\sqrt{2\pi}$ -Lipschitz continuity of the function Φ gives us

$$\text{BR}(h_\theta) \leq \frac{\varepsilon \|\theta\|_{\ell_2}}{\sqrt{2\pi} \|W^\top \theta\|_{\ell_2}}. \quad (24)$$

By writing the SVD of the weight matrix W we can get $W = USV^\top$. In this decomposition, matrices $U \in \mathbb{R}^{d \times k}$ and $V \in \mathbb{R}^{k \times k}$ have orthogonal rows, i.e. $U^\top U = V^\top V = I_k$, and S is a diagonal matrix with non-zero entries on its diagonal. From the range-kernel decomposition of matrix W , it is possible to decompose θ into two orthogonal components θ_0, θ_1 such that $\theta = \theta_0 + \theta_1$, $\theta_0^\top W = 0$, and there exists $\alpha \in \mathbb{R}^k$ such that $W\alpha = \theta_1$. By using the triangle inequality, we can get

$$\|\theta\|_{\ell_2} \leq \|\theta_0\|_{\ell_2} + \|W\alpha\|_{\ell_2}. \quad (25)$$

Further, we have (remember $V^\top V = I_k$):

$$\|W^\top \theta\|_{\ell_2} = \|W^\top W\alpha\|_{\ell_2} = \|S^2 V^\top \alpha\|_{\ell_2}. \quad (26)$$

By plugging (25), (26) into (24) we can get

$$\sqrt{2\pi} \text{BR}(h_\theta) / \varepsilon \leq \frac{\|W\alpha\|_{\ell_2}}{\|S^2 V^\top \alpha\|_{\ell_2}} \cdot \left(1 + \frac{\|\theta_0\|_{\ell_2}}{\|W\alpha\|_{\ell_2}}\right). \quad (27)$$

By using the fact that $U^\top U = I_k$, we can get $\|W\alpha\|_{\ell_2} = \|SV^\top \alpha\|_{\ell_2}$. This yields

$$\frac{\|W\alpha\|_{\ell_2}}{\|S^2 V^\top \alpha\|_{\ell_2}} = \frac{\|Sv^\top \alpha\|_{\ell_2}}{\|S^2 V^\top \alpha\|_{\ell_2}} \leq \frac{1}{\sigma_{\min}(S)}. \quad (28)$$

By recalling the condition number definition $\kappa(W) = \|W\| \|W^\dagger\|$, we have

$$1/\sigma_{\min}(S) = \kappa(W) / \sigma_{\max}(S) \leq \sqrt{k} \kappa(W) / \|W\|_F. \quad (29)$$

We combine (28) and (29) to get

$$\frac{\|W\alpha\|_{\ell_2}}{\|S^2 V^\top \alpha\|_{\ell_2}} \leq \frac{\kappa(W)}{\sigma_{\max}(S)} \leq \frac{\sqrt{k} \kappa(W)}{\|W\|_F} = o(1), \quad (30)$$

where the last equality is implied by (7). On the other hand, from (7), we have $\|\theta_0\|_{\ell_2} = o(\|\theta\|_{\ell_2})$. This relation combined with the fact that $\|\theta_0\|_{\ell_2}^2 + \|\theta_1\|_{\ell_2}^2 = \|\theta\|_{\ell_2}^2$ bring us $\|\theta_0\|_{\ell_2} = o(\|\theta_1\|_{\ell_2})$ hence

$$\|\theta_0\|_{\ell_2} / \|W\alpha\|_{\ell_2} = o(1). \quad (31)$$

Finally, deploying (30) and (31) in (27) completes the proof.

We now focus on the ERM problem. First, note that as the loss function ℓ is decreasing, it is easy to observe that the supremum of $yu^\top\theta$ over the adversarial ball $u \in B_\varepsilon(x_i)$ is $\ell(yx_i^\top\theta - \varepsilon\|\theta\|_{\ell_2})$. This implies that the adversarial ERM problem can be written as the following:

$$\arg \min_{\theta \in \mathbb{R}^d} R_n(\theta) := \frac{1}{n} \sum_{i=1}^n \ell(y_i x_i^\top \theta - \varepsilon \|\theta\|_{\ell_2}). \quad (32)$$

In order to show that the classifier $h_{\hat{\theta}^\varepsilon}$ has boundary risk converging to zero, we use the first part of the theorem. To this end, we need to show that the obtained solution $\hat{\theta}^\varepsilon$ will satisfy the conditions (7). We decompose $\hat{\theta}^\varepsilon$ into orthogonal components belonging to the kernel of matrix W^\top and the image of W . This implies $\hat{\theta}^\varepsilon = \theta_0 + \theta_1$ representation with $W^\top\theta_0 = 0$, and there exists $\alpha \in \mathbb{R}^k$ such that $\theta_1 = W\alpha$. We claim that indeed the kernel component of $\hat{\theta}^\varepsilon$ is zero, i.e. $\theta_0 = 0$. Assume $\theta_0 \neq 0$. By plugging $\theta = \theta_0 + \theta_1$ into (32) we get

$$\begin{aligned} R_n(\hat{\theta}^\varepsilon) &= \frac{1}{n} \sum_{i=1}^n \ell(y_i x_i^\top \hat{\theta}^\varepsilon - \varepsilon \|\hat{\theta}^\varepsilon\|_2) \\ &= \frac{1}{n} \sum_{i=1}^n \ell(y_i x_i^\top \theta_1 - \varepsilon \|\hat{\theta}^\varepsilon\|_2), \end{aligned}$$

where the last equality is followed by the fact that $x_i = Wz_i$ with $z_i \sim \mathcal{N}(y\mu_i, I_k)$, and $W^\top\theta_0 = 0$. Further, from the orthogonality of θ_0 and θ_1 we get

$$R_n(\hat{\theta}^\varepsilon) = \frac{1}{n} \sum_{i=1}^n \ell \left(y_i x_i^\top \theta_1 - \varepsilon \left(\|\theta_0\|_{\ell_2}^2 + \|\theta_1\|_{\ell_2}^2 \right)^{1/2} \right).$$

Finally, by using the fact that the loss function ℓ is a strictly decreasing function, and we assumed $\|\theta_0\|_{\ell_2} \neq 0$, we get

$$\begin{aligned} R_n(\hat{\theta}^\varepsilon) &> \frac{1}{n} \sum_{i=1}^n \ell \left(y_i x_i^\top \theta_1 - \varepsilon \|\theta_1\|_{\ell_2} \right) \\ &= R_n(\theta_1). \end{aligned}$$

It contradicts the initial assumption that $\hat{\theta}^\varepsilon$ is the minimizer of the $R_n(\theta)$. This means that $\theta_0 = 0$, and conditions (7) are satisfied.

5 Conclusion

In this paper, we studied the role of data distribution (in particular latent low-dimensional manifold structures of data) on the tradeoff between robustness (against adversarial perturbations in the

input, at test time) and generalization (performance on test data drawn from the same distribution as training data). We developed a theory for two widely used classification setups (Gaussian-mixture model and generalized linear model), showing that as the ratio of the ambient dimension to the manifold dimension grows, one can obtain models which both are robust and generalize well. This highlights the role of exploiting underlying data structures in improving robustness and also in mitigating the tradeoff between generalization and robustness. Through numerical experiments, we demonstrate that low-dimensional manifold structure of data, even if not exploited by the training method, can still weaken the robustness-generalization tradeoff.

Acknowledgement

A. Javanmard is partially supported by the Sloan Research Fellowship in mathematics, an Adobe Data Science Faculty Research Award and the NSF CAREER Award DMS-1844481.

References

- Biggio, B., Corona, I., Maiorca, D., Nelson, B., Srndić, N., Laskov, P., Giacinto, G., and Roli, F. (2013). Evasion attacks against machine learning at test time. In *Joint European conference on machine learning and knowledge discovery in databases*, pages 387–402. Springer. 1
- Carlini, N., Mishra, P., Vaidya, T., Zhang, Y., Sherr, M., Shields, C., Wagner, D., and Zhou, W. (2016). Hidden voice commands. In *25th {USENIX} Security Symposium ({USENIX} Security 16)*, pages 513–530. 1
- Costa, J. A. and Hero, A. O. (2004). Learning intrinsic dimension and intrinsic entropy of high-dimensional datasets. In *2004 12th European Signal Processing Conference*, pages 369–372. IEEE. 2
- Dobriban, E., Hassani, H., Hong, D., and Robey, A. (2020). Provable tradeoffs in adversarially robust classification. *arXiv preprint arXiv:2006.05161*. 2, 3
- Jalal, A., Ilyas, A., Daskalakis, C., and Dimakis, A. G. (2017). The robust manifold defense: Adversarial training using generative models. *arXiv preprint arXiv:1712.09196*. 3
- Javanmard, A. and Soltanolkotabi, M. (2020). Precise statistical analysis of classification accuracies for adversarial training. *arXiv preprint arXiv:2010.11213*. 2, 9
- Javanmard, A., Soltanolkotabi, M., and Hassani, H. (2020). Precise tradeoffs in adversarial training for linear regression. volume 125 of *Proceedings of Machine Learning Research, Conference of Learning Theory (COLT)*, pages 2034–2078. PMLR. 2
- Lin, W.-A., Lau, C. P., Levine, A., Chellappa, R., and Feizi, S. (2020). Dual manifold adversarial robustness: Defense against lp and non-lp adversarial attacks. In Larochelle, H., Ranzato, M., Hadsell, R., Balcan, M. F., and Lin, H., editors, *Advances in Neural Information Processing Systems*, volume 33, pages 3487–3498. Curran Associates, Inc. 3
- Madry, A., Makelov, A., Schmidt, L., Tsipras, D., and Vladu, A. (2018a). Towards deep learning models resistant to adversarial attacks. In *6th International Conference on Learning Representations, ICLR 2018, Vancouver, BC, Canada, April 30 - May 3, 2018, Conference Track Proceedings*. 2
- Madry, A., Makelov, A., Schmidt, L., Tsipras, D., and Vladu, A. (2018b). Towards deep learning models resistant to adversarial attacks. *arXiv preprint arXiv:1706.06083, International Conference on Learning Representations*. 3, 9
- Mehrabi, M., Javanmard, A., Rossi, R. A., Rao, A., and Mai, T. (2021). Fundamental tradeoffs in distributionally adversarial training. In *Proceedings of the 38th International Conference on Machine Learning*, volume 139, pages 7544–7554. PMLR. 2, 3
- Min, Y., Chen, L., and Karbasi, A. (2020). The curious case of adversarially robust models: More data can help, double descend, or hurt generalization. *arXiv preprint arXiv:2002.11080*. 2, 3
- Raghunathan, A., Xie, S. M., Yang, F., Duchi, J. C., and Liang, P. (2019). Adversarial training can hurt generalization. *arXiv preprint arXiv:1906.06032*. 2, 3

- Rozza, A., Lombardi, G., Ceruti, C., Casiraghi, E., and Campadelli, P. (2012). Novel high intrinsic dimensionality estimators. *Machine learning*, 89(1):37–65. [2](#)
- Song, Y., Shu, R., Kushman, N., and Ermon, S. (2018). Constructing unrestricted adversarial examples with generative models. In Bengio, S., Wallach, H., Larochelle, H., Grauman, K., Cesa-Bianchi, N., and Garnett, R., editors, *Advances in Neural Information Processing Systems*, volume 31. Curran Associates, Inc. [3](#)
- Spigler, S., Geiger, M., and Wyart, M. (2020). Asymptotic learning curves of kernel methods: empirical data versus teacher–student paradigm. *Journal of Statistical Mechanics: Theory and Experiment*, 2020(12):124001. [2](#)
- Stutz, D., Hein, M., and Schiele, B. (2019). Disentangling adversarial robustness and generalization. In *Proceedings of the IEEE/CVF Conference on Computer Vision and Pattern Recognition*, pages 6976–6987. [3](#)
- Szegedy, C., Zaremba, W., Sutskever, I., Bruna, J., Erhan, D., Goodfellow, I., and Fergus, R. (2014). Intriguing properties of neural networks. *International Conference on Learning Representations (ICLR)*. [1](#)
- Tsipras, D., Santurkar, S., Engstrom, L., Turner, A., and Madry, A. (2018). Robustness may be at odds with accuracy. *arXiv preprint arXiv:1805.12152*. [3](#)
- Vaidya, T., Zhang, Y., Sherr, M., and Shields, C. (2015). Cocaine noodles: exploiting the gap between human and machine speech recognition. In *9th {USENIX} Workshop on Offensive Technologies ({WOOT} 15)*. [1](#)
- Xing, Y., Zhang, R., and Cheng, G. (2021). Adversarially robust estimate and risk analysis in linear regression. In *International Conference on Artificial Intelligence and Statistics*, pages 514–522. PMLR. [2](#)
- Yang, Y.-Y., Rashtchian, C., Zhang, H., Salakhutdinov, R. R., and Chaudhuri, K. (2020). A closer look at accuracy vs. robustness. In Larochelle, H., Ranzato, M., Hadsell, R., Balcan, M. F., and Lin, H., editors, *Advances in Neural Information Processing Systems*, volume 33, pages 8588–8601. Curran Associates, Inc. [2](#), [3](#)
- Zhang, G., Yan, C., Ji, X., Zhang, T., Zhang, T., and Xu, W. (2017). Dolphinattack: Inaudible voice commands. In *Proceedings of the 2017 ACM SIGSAC Conference on Computer and Communications Security*, pages 103–117. [1](#)
- Zhang, H., Yu, Y., Jiao, J., Xing, E. P., Ghaoui, L. E., and Jordan, M. I. (2019). Theoretically principled trade-off between robustness and accuracy. In *Proceedings of the 36th International Conference on Machine Learning, ICML 2019, 9-15 June 2019, Long Beach, California, USA*, pages 7472–7482. [2](#), [3](#)